



HAL
open science

Impact of inflated structures on a liquid free surface.

S. Halbout, Nicolas Malleron, Fabien Remy, Yves-Marie Scolan

► **To cite this version:**

S. Halbout, Nicolas Malleron, Fabien Remy, Yves-Marie Scolan. Impact of inflated structures on a liquid free surface.. 23rd International Workshop on Water Waves and Floating Bodies, Apr 2009, Zelenogorsk, Russia. 4pp. hal-00458073

HAL Id: hal-00458073

<https://hal.science/hal-00458073>

Submitted on 19 Feb 2010

HAL is a multi-disciplinary open access archive for the deposit and dissemination of scientific research documents, whether they are published or not. The documents may come from teaching and research institutions in France or abroad, or from public or private research centers.

L'archive ouverte pluridisciplinaire **HAL**, est destinée au dépôt et à la diffusion de documents scientifiques de niveau recherche, publiés ou non, émanant des établissements d'enseignement et de recherche français ou étrangers, des laboratoires publics ou privés.

Impact of inflated structures on a liquid free surface.

S. Halbout*, N. Malleron*, F. Remy**, Y.-M. Scolan**,

* Eurocopter, Aeroport Marseille-Provence, 13700 Marignane, France

** Centrale Marseille – IRPHE CNRS, France, severin.halbout@ec-marseille.fr

1) Introduction

There are many situations where inflated structures may hit violently a liquid free surface. One of them occurs during sea-landing of helicopters. As a matter of fact helicopters are equipped with inflated floaters. Those floaters are made of impermeable tissues which are almost inextensible and their flexural rigidity is small. These mechanical characteristics are difficult to reproduce at model scales, that is why we found more conventional inflated balloons like space hopper. Definitely they have different mechanical properties than actual floaters. In spite of these differences, experiments have been carried out in the flume of Ecole Centrale Marseille. Only qualitative measurements have been performed. High speed camera provided the main features of the phenomenon.

This abstract sums up this experimental campaign and the first attempts done in the numerical modellings thus yielding some comparisons. It is shown that simple linearized models –both structural and hydrodynamic models – can reproduce the early stage of penetration when impact occurs. Those give initial conditions for new models which are expected to reproduce the beginning of the water exit.

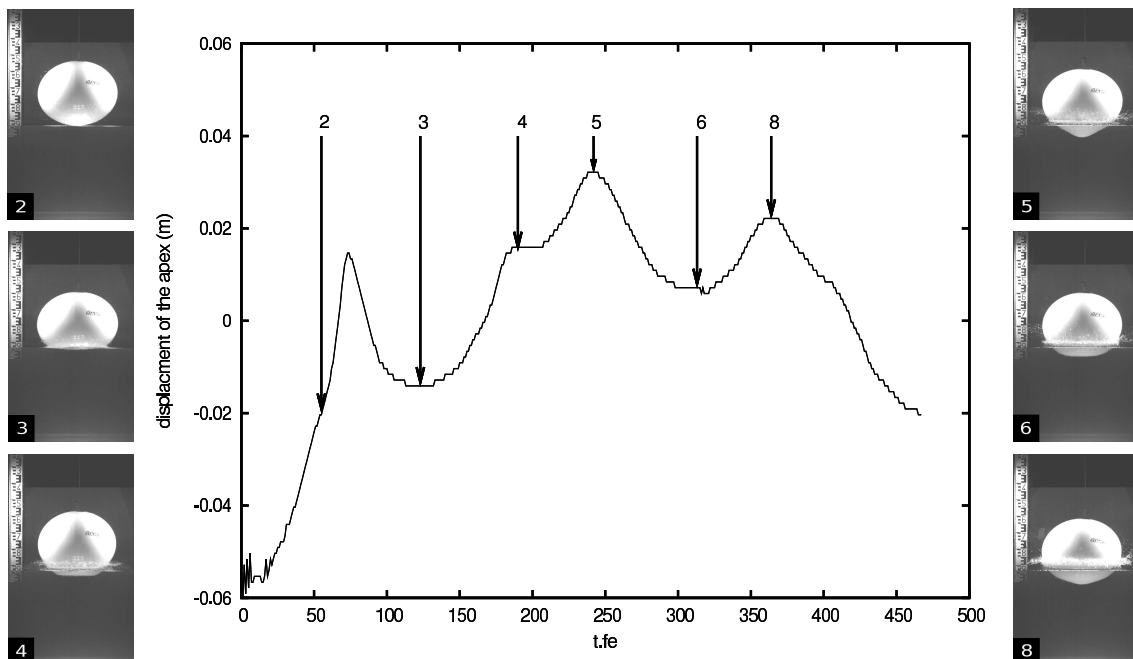
2) Experimental campaign

Free drop tests are performed. The figure below shows three elements of the set-up.



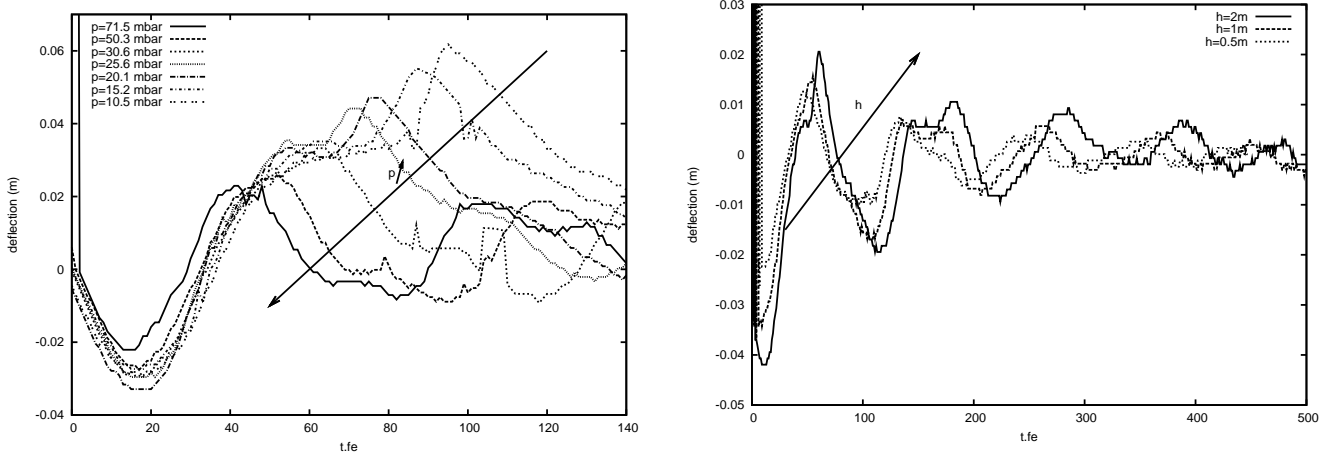
A floater (left) falls over a height h onto an initial flat free surface. A fast camera (center) records the final stage of the drop in air and the whole fluid-structure interaction up to a possible rebound. The camera works at 1000 frames per second. The water is coloured with fluorescein (right) in order to improve the diffusion of light into the liquid. Analysis of the video recording provides most of the data for the parametric study.

The penetration of the balloon into the liquid is broken down into two phases of several steps. Those are summed up in the following sketch



The central figure shows the time variation of the position of the lower point corresponding to the initial contact point: this point is noted *A* in the sequel. From step 2 to step 3, the floater undergoes a fast deceleration. The following steps correspond to a phase of oscillation of the wetted surface, whereas its size hardly varies. As these data follows from image analysis, when point *A* is not visible, we cannot determine its position, that occurs at step 4. The final stage (not shown here) is the rebound.

The parameters are limited to the initial drop height (giving the velocity at initial contact) and the pressure p_{int} inside the balloon (controlling the mechanical characteristics of the elastic membrane). The influences of these two parameters are illustrated below



These are the time variations of the vertical position of point *A* for different inner pressures and drop heights. It is noted that the first stages of penetration are quite similar whatever the values of the parameters. When oscillation phase starts, the influence of parameters are more noticeable. In the left figure, the arrow indicates the increasing inner pressure. It is worth noting that the smaller the inner pressure, the greater the deflection of point *A*, as if this point was "sucked" in the liquid. In the right figure the arrow indicates the increasing drop height for a given inner pressure. The figure shows that increasing the initial velocity just leads to amplify the magnitude of the deflection whereas the frequency of oscillations is hardly affected.

3) Dimensional analysis

A dimensional analysis shows that three dimensionless numbers are of importance. These numbers are calculated for the following data: diameter of the space hopper: $D = 0.46m$ (it is supposed to be spherical), Young modulus: $E = 302MPa$, Poisson coefficient: $\nu = 0.31$ and density: $\rho_s = 1060Kg/m^3$. The average thickness is $H = 1.1mm$. The following table sums up the calculated numbers depending on the identified phases of the fluid structure interaction:

	numbers	initial phase	oscillation phase
$\frac{w}{R} = f \left(\frac{p_{int}}{\rho_f V_f^2}, \frac{\rho_f V_f^2}{E}, \frac{V_f}{V_s} \right)$	Euler number $\frac{p_{int}}{\rho_f V_f^2}$	$O(10^{-3})$	$O(1)$
	Cauchy number $\frac{\rho_f V_f^2}{E}$	$O(10^{-1})$	$O(10^{-6})$
	reduced velocity $\frac{V_f}{V_s}$	$O(1)$	$O(10^{-2})$

where indices f and s refer to the fluid and the solid respectively. w is the deflection and R the radius of the sphere. The scale velocity of the fluid is denoted V_f ; it follows from the evaluation of the velocity of expansion of the wetted surface and therefore it is significant during the initial phase. During the oscillation phase it is set to unity. The scale velocity in the structure follows from the formula $V_s = \sqrt{\frac{E}{\rho_s}}$. We conclude that fluid structure interactions mainly occur during the initial phase. Later during the oscillation phase, we deal with a spherical cup initially deformed (initial potential energy) and hence it is oscillating. The mechanism which leads to a rebound is not detailed here.

4) Modelings

In order to describe the early stage of penetration, simple linearized models may suffice. From the theoretical developments detailed in Scolan (2004) the elaborated model combines a Wagner model (1932) and a linear

elastic model for thin shell. The configuration is fully axisymmetric. That means that the floater is locally represented at the initial contact point A as a paraboloid with a radius of curvature R . This radius R is supposed to be large compared to the penetration depth. The linearization of the boundaries follows the assumption that deadrise angle is small. Hence the shell is considered as a flat disk. All variables are broken down as series of normal modes, for example the deflection is written as

$$w(x, y, t) = \sum_n^{\infty} A_n(t) w_n(x, y) \quad (1)$$

The mode shape w_n depend on the boundary conditions and they are expressed with Bessel functions of zeroth order. For the present application we considered a disk clamped along its outer boundary: only J_0 and I_0 are used. It is shown that the value of the outer radius has a light influence on the results: here we take an outer radius $0.5m$ and the series contain 20 modes.

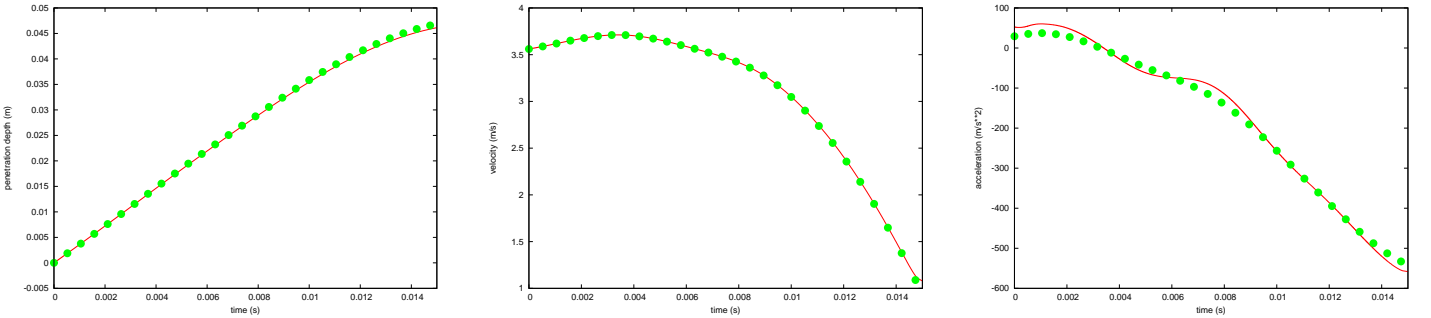
The hydrodynamic boundary value problem is formulated in term of displacement potential. The solution is Hankel transformed. Wagner condition stipulates that the vertical displacement at the contact line is finite and that yields an equation for the position of this contact line which reads

$$\sum_n A_n Q_n = \int_0^t V(\tau) d\tau - \frac{a^2}{3R}, \quad \text{with} \quad Q_n(a) = \int_0^{\pi/2} \sin \theta w_n(a(t) \sin \theta) d\theta \quad (2)$$

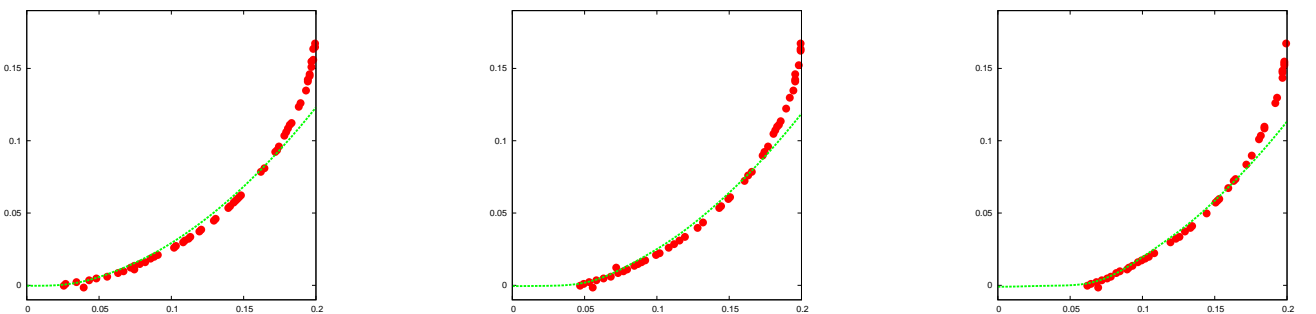
where $a(t)$ denotes the radius of the contact line. From Sneddon (1966) the velocity potential φ can be expressed in a closed form as

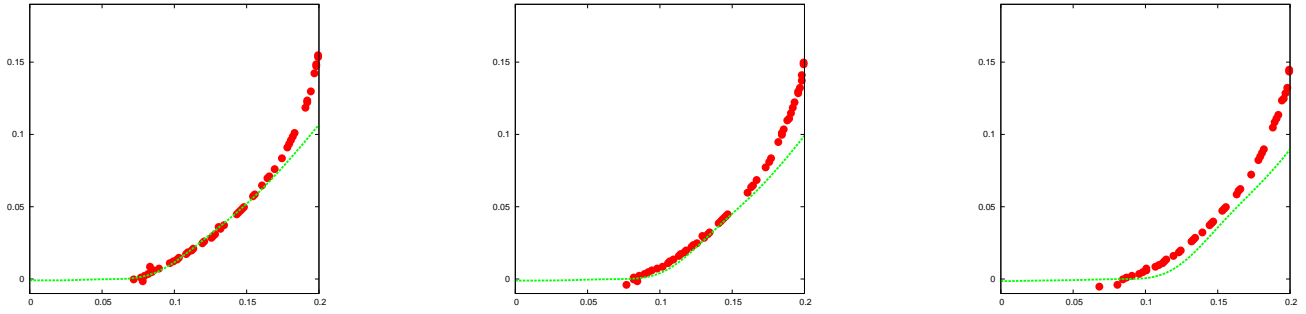
$$\varphi(r, a) = -\frac{2V(t)}{\pi} \sqrt{a^2 - r^2} + \sum_n \dot{A}_n \Phi_n, \quad \text{with} \quad \Phi_n(r, a) = \frac{2r}{\pi} \int_0^{\text{argch}(a/r)} \cosh x Q_n(r \cosh x) dx. \quad (3)$$

where $V(t)$ denotes the instantaneous velocity of penetration and r is the radial coordinate. A time differential system for a and A_n is formulated and solved. If free drops are considered, Newton law closes the system of equations. In the present application, instead of letting the floater freely penetrating the liquid, we impose its kinematics. That means that the time history of V is given and follows from experiments. The following figures show the time variations of penetration depth (left), velocity (center) and acceleration (right).

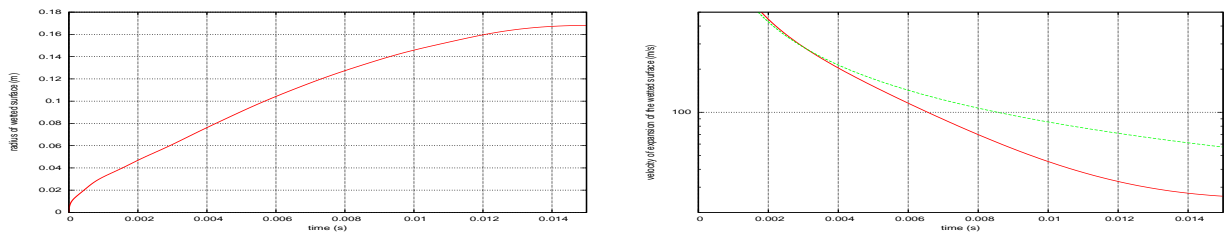


The computations provide the deformed shapes at some discrete instants (roughly at the first six milliseconds, those are plotted below (solid lines) and compared to measured data (dots))





It is clear that during the first stage of penetration (up to $t \approx 6ms$) the present model accurately predicts the size of the wetted surface and its expansion. In particular the fact that the wetted surface becomes almost flat is well reproduced. The following figures show the time variation of the radius of the wetted surface and its time derivative. In the right figure both rigid case ($da/dt = \frac{3RV}{2a}$) and present elastic case are drawn



The theoretical singular behavior of the velocity da/dt at the first instant of contact is clear; actually da/dt behaves like $1/\sqrt{t}$. These consideration are of some interest since the maximum of pressure varies as the square of the expansion velocity and consequently the predicted pressure distribution by the present model might be somewhat unrealistic.

In order to describe the latter stages of penetration, the present model fails since this model still predicts an expansion of the wetted surface as experiments show that the wetted surface varies slightly and the oscillation phase starts. Adapted models can be elaborated on the basis of the present one and for which we can consider that the wetted surface is more or less at rest. Future works are oriented towards this direction.

5) Conclusion

We consider the free fall of an inflated floater onto a initial flat free surface of water. Some qualitative experimental results are obtained by means of fast video recordings. The expansion of the wetted surface and the deformed shape are well predicted during the early stages of penetration. Much works are still to be done.

Experimentally the inner pressure should be measured, that would help to better understand the coupling with the inner compressed gas. Comparisons with the impact of the floaters onto a solid ground should be done. Finally the phenomenon should be observed from below, in order to check the axisymmetry on one hand and to better measure the expansion of the wetted surface, on the other hand.

Numerically, it is expected that a Generalized Wagner Model for elastic shell should improve the results. Then the oscillation phase can be better reproduced and the hence the conditions under which a rebound occurs.

6) References

1. Scolas Y.-M., 2004, Hydroelastic behaviour of a conical shell impacting on a quiescent-free surface of an incompressible liquid. *Journal of Sound and Vibration* . Volume 277, Issues 1-2, pp 163-203.
2. Sneddon I.N., 1966 Mixed boundary value problems in potential theory. J. Wiley & Sons, Inc.
3. Wagner H. 1932 Über Stoss- und Gleitvorgänge an der Oberfläche von Flüssigkeiten. *ZAMM* **12**, 193-215.